Optimizing the Stroke of Purcell's Rotator, a Low Reynolds Number Swimmer

by

Victoria N. Hammett

Submitted to the Department of Mechanical Engineering
in partial fulfillment of the requirements for the degree of

Bachelor of Science in Mechanical Engineering

at the

MASSACHUSETTS INSTITUTE OF TECHNOLOGY

June 2012

Author .....
Department of Mechanical Engineering
May 10, 2012

Certified by .....
Anette Hosoi
MacVicar Faculty Fellow, Associate Professor of Mechanical Engineering
Thesis Supervisor

Accepted by .....
John H. Lienhard V
Samuel C. Collins Professor of Mechanical Engineering
Undergraduate Officer

Optimizing the Stroke of Purcell's Rotator, a Low Reynolds Number Swimmer

by

Victoria N. Hammett

Submitted to the Department of Mechanical Engineering
on May 10, 2012, in partial fulfillment of the
requirements for the degree of

Bachelor of Science in Mechanical Engineering

Abstract

Purcell's rotator is a theoretical low Reynolds number swimmer that can act as a model of more complex natural microorganisms, such as *E.coli.* Because of the low Reynolds number environment, the swimmer has approximately no inertia and it's motion is dominated by viscous forces. The version of Purcell's rotator examined in this paper is two dimensional and has three rigid links which rotate about the center of the body. It is able to propel itself by moving these links in a repetitive, nonreciprocal stroke motion. Using a mathematical model of the swimmer, two strokes were found, one which optimizes its rotation of the swimmer and one which optimizes its translation.

Thesis Supervisor: Anette Hosoi
Title: MacVicar Faculty Fellow, Associate Professor of Mechanical Engineering

Acknowledgments

The author would like to thank Professor Anette Hosoi of the Department of Mechanical Engineering at the Massachusetts Institute of Technology for her assistance and sponsorship throughout this project. The author would also like to thank Lisa Burton, also of the MIT Mechanical Engineering, for her unceasing assistance and advice.

Contents

List of Figures

Chapter 1

Introduction

This project aims to find two optimized strokes of Purcell's rotator, a theoretical low Reynolds number swimmer. This swimmer serves as a model for low Reynolds number swimmers found in nature, which are generally unicellular organisms like bacteria or yeast. The low Reynolds number environment is such that inertial forces cease to be a major factor in their motion, which is dominated by viscous forces.

Purcell's rotator is a simplified model of a locomoting microorganism. The version of Purcell's rotator that will be investigated consists of three rigid links which are connected in the center of the organism. The articulation of these links will be optimized to find strokes which allow for maximum rotation and translation of the swimmer.

1.1 Low Reynolds Number Swimmers

The ratio of inertia forces to the viscous forces acting on a body is represented by the Reynolds number. It is expressed as $Re = \frac{\rho v d}{\mu}$ where ρ is the density of the surrounding fluid, v is the velocity of the body, d is the length of the body, and μ is the viscosity of the surrounding fluid. A high Reynolds number corresponds to high inertia forces acting on the body, and a low Reynolds number corresponds to high viscous forces.

We spend most of our existence in a high Reynolds number realm, where our

movement largely depends on our inertia. However, by examining the low Reynolds number realm, defined by small length scales as well as small velocities, we can expose a much different environment. In this case, inertia is so small that it may be neglected and instead, viscous forces largely dominate the motion of organisms. Additionally, at low Reynolds numbers, time can be scaled out of the equations of motion such that reversible motions will not produce any net translation [3]. This is demonstrated by the motion of a scallop - a high Reynolds number swimmer, which moves by opening its one hinge slowly and closing it quickly. This reciprocal motion at a low reynolds number would simply pull the scallop back then push it forward, returning it to its initial position [6]. Instead, during a stroke, a microorganism must return to its original configuration using a different path than it took to get there [2]. Thus, in order to have nonreciprocating motion, all low Reynolds number swimmers must also have at least two degrees of freedom.

These microorganisms are in fact very important in sustaining life. The organisms which are small enough to qualify for life at a low Reynolds number make up the base of the food web and produce almost half of the world's oxygen [3]. Understanding their mode of locomotion is therefore beneficial. Optimizing the stroke of a simplified swimmer will help us understand these organisms.

In this paper we will discuss low Reynolds numbers where $Re < 10^{-4}$, and therefore assume that $Re \ll 1$. While some low Reynolds number swimmers are multicellular, they are typically single cell organisms with lengths on the order of 100 μm [6]. Some organisms that fall in this region are *E. Coli*, algae, or yeast.

1.2 Purcell's Rotator

We will be looking specifically at Purcell's rotator. Purcell's rotator is a theoretical low Reynolds number swimmer proposed by E. M. Purcell. It is a two dimensional system comprised of three spheres connected by links at the center of the body. These spheres are attached by perfectly rigid, massless links which create no drag. However, for this study, a variation of Purcell's rotator was examined. This version

has no spheres but instead consists of three links, joined in the center. These links are perfectly rigid and do create drag, allowing the swimmer to propel itself.

Purcell's rotator, unlike a scallop, has two degrees of freedom, and is therefore able to produce net motion in a low Reynolds number environment using a nonreciprocating gait. By determining the forces produced by the organism when actuating the links about its center, it is possible to find the optimum stroke. This stroke will be developed for rotation and translation, together filling the entire space of motion. This theoretical swimmer differs from actual organisms observed in nature. Specifically, the links are rigid, unlike most flagella, which create motion by propagating waves down their length. Ultimately, differences between this swimmer and natural swimmers will be observed.

Chapter 2

Background

We will first examine geometry of the swimmer and the forces acting on the it. These will be used to develop the local connection matrix and the reconstruction equation which describe the swimmer's motion.

2.1 Low Reynolds Number Flows

We can make a few assumptions due to the fact that Purcell's rotator exists in a low Reynolds number environment. We can examine the Navier-Stokes equation which is generally expressed as

$$\rho \frac{D\overrightarrow{v}}{Dt} = -\nabla P + \rho \overrightarrow{g} + \mu \nabla^2 \overrightarrow{v} \tag{2.1}$$

for fluid density ρ, body velocity v, pressure P, gravity g, and fluid viscosity μ. However, assuming $Re \ll 1$ and without gravity acting on the two dimensional system, Equation 2.1 becomes

$$0 = -\nabla P + \mu \nabla^2 \overrightarrow{v}. \tag{2.2}$$

Equation 2.2, Stokes equation, therefore allows us to disregard inertia. Additionally, the Navier-Stokes equation no longer contains time explicitly and reciprocal stokes will no longer create a net displacement. We will also assume that Purcell's

rotator is a two dimensional body moving through in two dimensional space. Furthermore, it is assumed that the links are very slender. Using resistive force theory for a very slender body [1] we can express the force on each individual link as

$$\begin{bmatrix} F_x \\ F_y \end{bmatrix} = \begin{bmatrix} 1 & 0 \\ 0 & 2 \end{bmatrix} \begin{bmatrix} v_x \\ v_y \end{bmatrix} \tag{2.3}$$

This will be further discussed in Section 2.3, in which the forces acting on the body will be examined.

2.2 Geometry of Purcell's Rotator

To describe the geometry of Purcell's Rotator, we will define the head of the swimmer and the tail of the swimmer. The tail of the swimmer is composed of two links which can be seen in Figure 2-1.

These three links are all identical, with a length L and a thickness R where $R \ll L$. The overall rotation of the swimmer is described by θ, the angle of the head. The x and y movement of the swimmer in the world frame is determined by the position of the center of the swimmer, point p. The position of the tail is described by line a, which bisects the two tail links. The angle α_1 is defined as the angle between the head link and line a, as seen in Figure 2-1. It describes the rotation of the two tail links with respect to the head of the swimmer.

The angle α_2 describes the angle between the two tail links. It is determined by the angle between an individual tail link and the line a, such that α_2 is equal to the angle between the link and line $a - 60°$. This relation can be seen in Figure 2-2. When all three links are evenly spaced, α_1 and α_2 are equal to 0.

The motion of the rotator is constrained by its geometry, specifically, the three links cannot cross. This leads to three different constraints that were taken into account during the optimization. First, α_1 cannot be smaller than $\frac{-\pi}{3}$. This would result in the two tail links interfering. Next, to avoid tail a from interfering with the head link, we impose that $\alpha_2 - \alpha_1 + \frac{\pi}{3} < \pi$. Additionally, to avoid interference

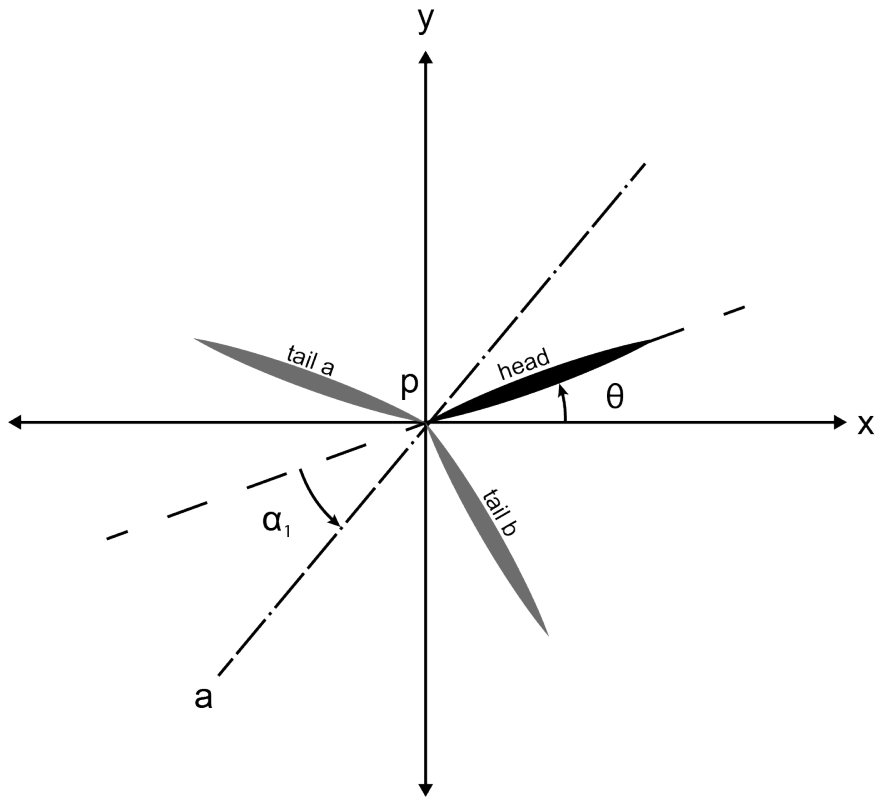

Figure 2-1: Purcell's rotator consists of a head and two tail links (grey). The position of the swimmer is determined by the point p. α_1 describes the rotation of the tail with respect to the head.

between tail b and the head, $\alpha_2 + \alpha_1 + \frac{\pi}{3} < \pi$. Figure 2-3 shows the different shapes that the rotator can make, with respect to α_1 and α_2, as well as the boundaries of the possible shapes.

Using the geometry of Purcell's rotator, as well as the physical constraints of its motion, we can describe the forces acting on the links in order to define its velocity and translation.

2.3 Motion of Purcell's Rotator

To determine the optimal stroke of the rotator, we must first describe its motion. First, the velocity of the links are described in each link's individual reference frame, with the x-axis aligned with the link. Assuming resistive force theory for very slender

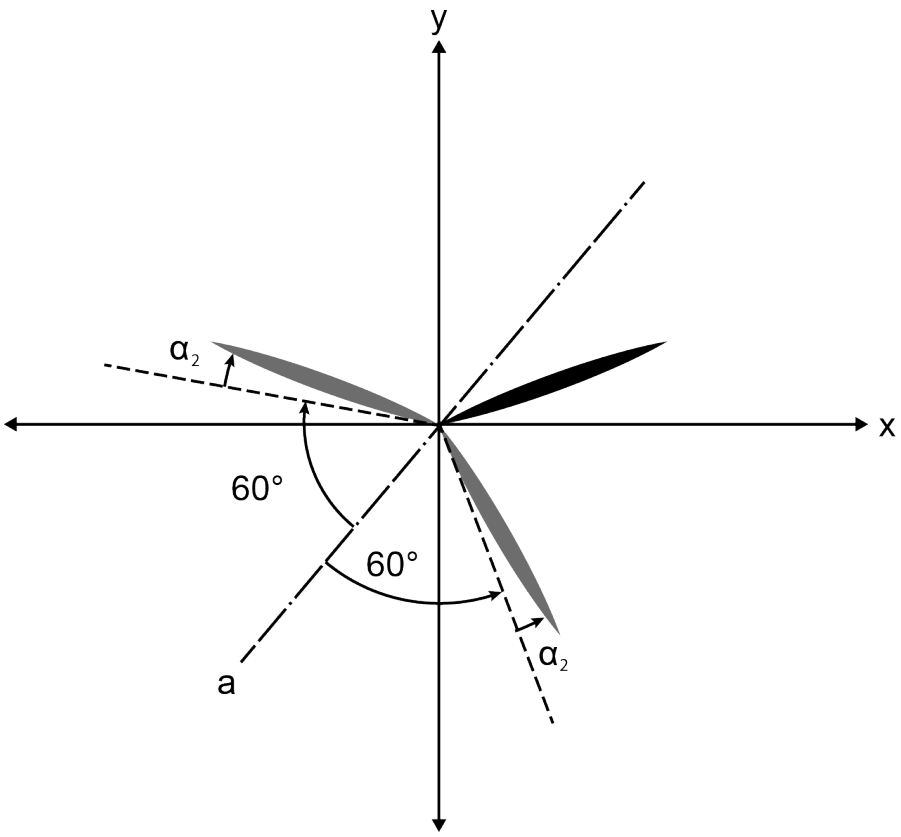

Figure 2-2: The angle α_2 describes the angle between the two tail links. When α_2 is 0, the two tail links are 120° apart.

links, the force on the link is proportional to the link velocity, such that the force perpendicular to the link is twice the force in the tangent direction, as expressed in Equation 2.3.

These forces can be translated into the reference frame of the head and summed to find the total force on the body described by velocity in the x and y directions, $\dot{x}$ and $\dot{y}$; the angular velocity, $\dot{\theta}$, α_1 and α_2, as well as $\dot{\alpha_1}$ and $\dot{\alpha_2}$. This process is repeated for the torque on the system. Because we assume there is no inertia, these forces sum to zero.

$$0 = \Sigma F_x = F_x(\dot{x}, \dot{y}, \dot{\theta}, \dot{\alpha_1}, \dot{\alpha_2}) \tag{2.4a}$$

$$0 = \Sigma F_y = F_y(\dot{x}, \dot{y}, \dot{\theta}, \dot{\alpha_1}, \dot{\alpha_2}) \tag{2.4b}$$

$$0 = \Sigma T = T(\dot{x}, \dot{y}, \dot{\theta}, \dot{\alpha_1}, \dot{\alpha_2}) \tag{2.4c}$$

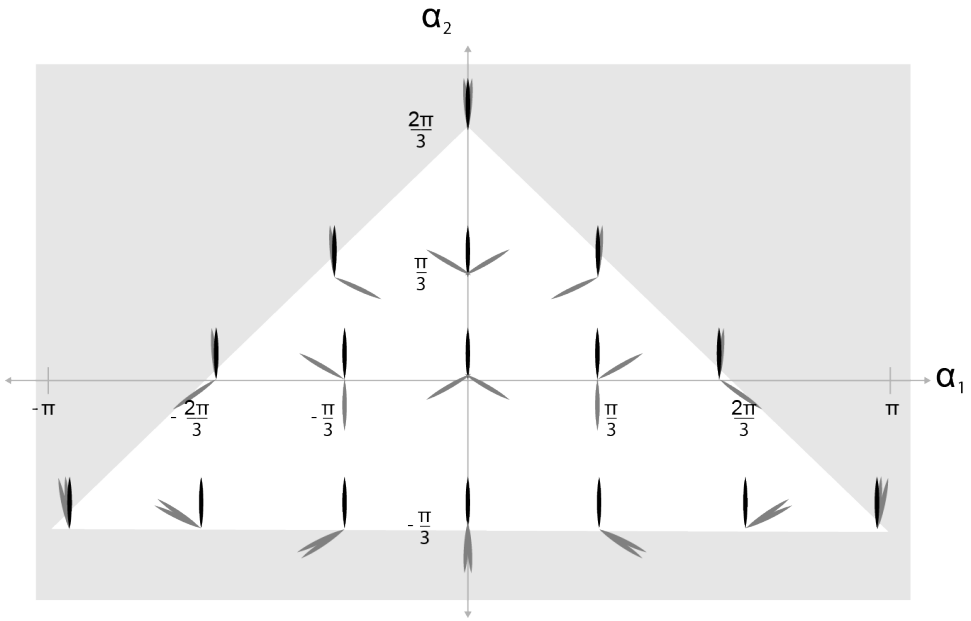

Figure 2-3: The possible configurations are within the white area. It is notable that at $\alpha_1 = \alpha_2 = 0$ the links are evenly spaced. The swimmer collapses in three configurations at the corners of the available space

Thus we can express Equation 2.4 in matrix form as seen below in Equation 2.5, where D is a 3 x 5 matrix populated with functions of α_1 and α_2

$$0 = \begin{bmatrix} F_x \\ F_y \\ T \end{bmatrix} = D \begin{bmatrix} \dot{x} \\ \dot{y} \\ \dot{\theta} \\ \dot{\alpha_1} \\ \dot{\alpha_2} \end{bmatrix} \tag{2.5}$$

We can then break D into two matrices, M_1, a 3x3 matrix, and M_2, an 3x2 matrix such that

$$0 = \begin{bmatrix} F_x \\ F_y \\ T \end{bmatrix} = M_1 \begin{bmatrix} \dot{x} \\ \dot{y} \\ \dot{\theta} \end{bmatrix} + M_2 \begin{bmatrix} \dot{\alpha_1} \\ \dot{\alpha_2} \end{bmatrix} \tag{2.6}$$

Solving for the velocity of the swimmer, we find the reconstruction equation,

$$\begin{bmatrix} \dot{x} \\ \dot{y} \\ \dot{\theta} \end{bmatrix} = -M_1^{-1} M_2 \begin{bmatrix} \dot{\alpha_1} \\ \dot{\alpha_2} \end{bmatrix} = A \begin{bmatrix} \dot{\alpha_1} \\ \dot{\alpha_2} \end{bmatrix} \tag{2.7}$$

Where A is the local connection matrix depending on α_1 and α_2, as well as the length of the links, L, and their width, R. Matrix A describes the geometry of the the swimmer as well as the forces acting on it, and can be used to optimize the stroke of the swimmer. Finding the series of α_1 and α_2 movements that result in a local connection matrix to maximize displacement or rotation will allow us to optimize the stroke.

Chapter 3

Stroke Optimization

Using Mathematica and MATLAB, optimal strokes in terms of displacement per unit cycle, or speed, were found for both rotation and translation. These strokes were represented by two Fourier series for α_1 and α_2.

3.1 Optimization Process

In order to find the series of movements in α_1 and α_2 which produced the best strokes for rotation and translation, the optimal local connection matrix A, as described in Equation 2.7 was found. The expression for A in terms of α_1 and α_2 was done by developing equations 2.4 through 2.7 in Mathematica. The stroke of the swimmer is defined as a Fourier series, specifically, α_1 and α_2 are expressed as

$$\alpha_1(t) = a_0^1 + a_1^1\cos(t) + a_2^1\sin(t) + a_3^1\cos(2t) + a_4^1\sin(2t) + ... \tag{3.1a}$$

$$\alpha_2(t) = a_0^2 + a_1^2\cos(t) + a_2^2\sin(t) + a_3^2\cos(2t) + a_4^2\sin(2t) + ... \tag{3.1b}$$

The stroke of the system was found using framework developed and further described by Hatton and Choset (2011) [4],[5]. Initially, optimized coordinates for the system were found. The body velocity of the swimmer is found using the reconstruction equation, as described in Equation 2.7. Applying Stokes' theorem to the local

connection matrix allows us to develop a series of height functions, which describe the net motion over the shape space. The total displacement of the swimmer is represented by the integral of the height function over the curve described by the stroke. Finally, the ideal gait was optimized using MATLAB's *fmincon* function. For rotation, this function was θ and for translation the function was y, using the system's optimized coordinates.

3.2 Optimized Rotation Stroke

The optimized rotation stroke encircles a peak in the θ height function to maximize rotation. Figure 3-1 shows the levels of the height function (orange), overlaid with the optimized stroke (bold blue). The stroke starts at $\alpha_1 = 0$ and $\alpha_2 = 1.917$ and moves counterclockwise in the shape space, hugging the boundary described by $\alpha_2 + \alpha_1 < \frac{2\pi}{3}$. In this configuration, the head link and tail link a stay stationary while tail link b moves in a counterclockwise direction. This movement continues until the gait reaches the zero contour line, at which point, the swimmer begins to follow that path. Following the zero contour maximizes the rotational displacement by encompassing the largest amount of negative displacement. The stroke then finds the boundary defined by $\alpha_2 - \alpha_1 < \frac{2\pi}{3}$ and follows it up to the starting point, by keeping the head link and tail link b stationary, while tail link a rotates in a clockwise direction.

The optimized stroke can be expressed as a Fourier series.

$$\alpha_1(t) = 0 + 1.4961\sin(t) - 0.4335\sin(2t) - 0.1011\sin(3t) - 0.0674\sin(4t) \tag{3.2a}$$

$$\alpha_2(t) = 0.2855 + 1.5035\cos(t) + 0.1515\cos(2t) - 0.9686\cos(3t) + 0.0464\cos(4t) \tag{3.2b}$$

It is notable that this gait is not a reciprocal motion, which would create no net

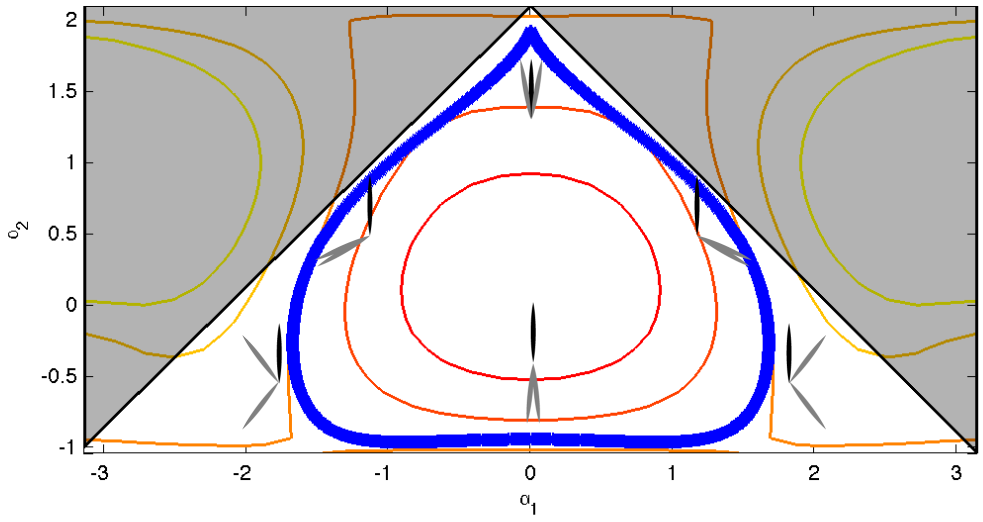

Figure 3-1: Height function for rotation is shown by the orange contours. There is a minimum in the height function near $\alpha_1 = \alpha_2 = 0$. The gait of the rotator is shown with the blue line, moving counterclockwise in the shape space, encompassing the minimum. The grey area represents impossible configurations.

displacement at low Reynolds number. Instead, the swimmer returns to its starting point using a different motion.

The optimized rotation stroke can be compared to a more simple stroke which is a circle in the shape space, defined by

$$\alpha_1(t) = \frac{\pi}{1+\sqrt{2}}\cos(t) \tag{3.3a}$$

$$\alpha_2(t) = -\frac{\pi}{3} + \frac{\pi}{1+\sqrt{2}} + \frac{\pi}{1+\sqrt{2}}\sin(t) \tag{3.3b}$$

This simple stroke is seen in Figure 3-2. It is found that the optimized stroke produces a net rotation 1.16 times greater than the simple stroke. Thus, the optimized

gait is able to increase the rotation.

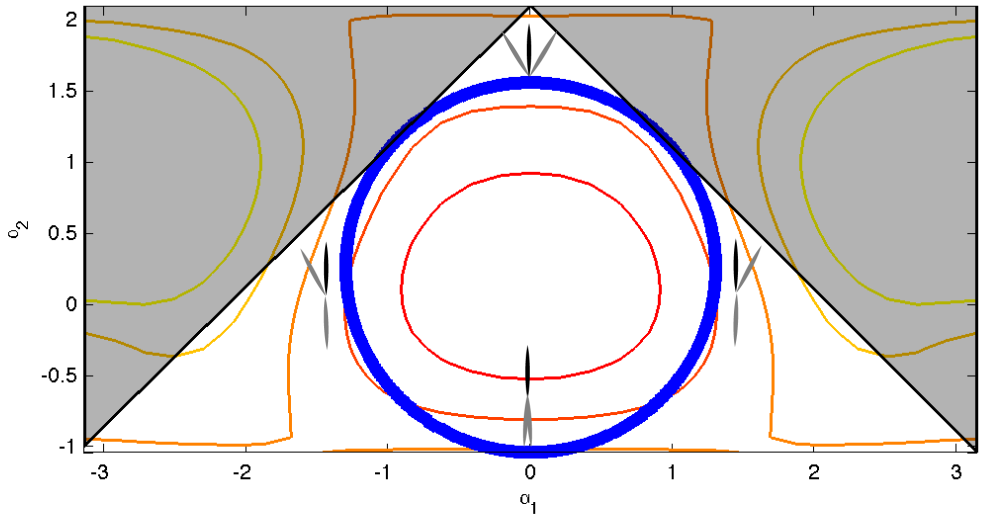

Figure 3-2: Height function for rotation is shown by the orange contours. A simple circular stroke is proposed to be compared to the optimized rotation stroke.

3.3 Optimized Translation Stroke

A stroke which optimizes translation of the swimmer was also found. The objective function in this case translation in the y direction for the systems optimized coordinates . This stroke moves counterclockwise through the shape space, encompassing the positive peak at $\alpha_1 = 0$. The gait begins with all three links together and begins to follow near the zero contour line, as tail link b opens counterclockwise. For the translation stroke it does not exactly follow the zero contour because the swimmer continues to experience rotation throughout the stroke, effecting its translation. The two tail links then meet at $\alpha_1 = 0$, followed by tail link a swinging in a clockwise

direction, and finally, all three links collapsing the the starting position. The progression of this stroke can be seen in Figure 3-3. Again, the height function is represented by the orange contours while the gait is seen in blue.

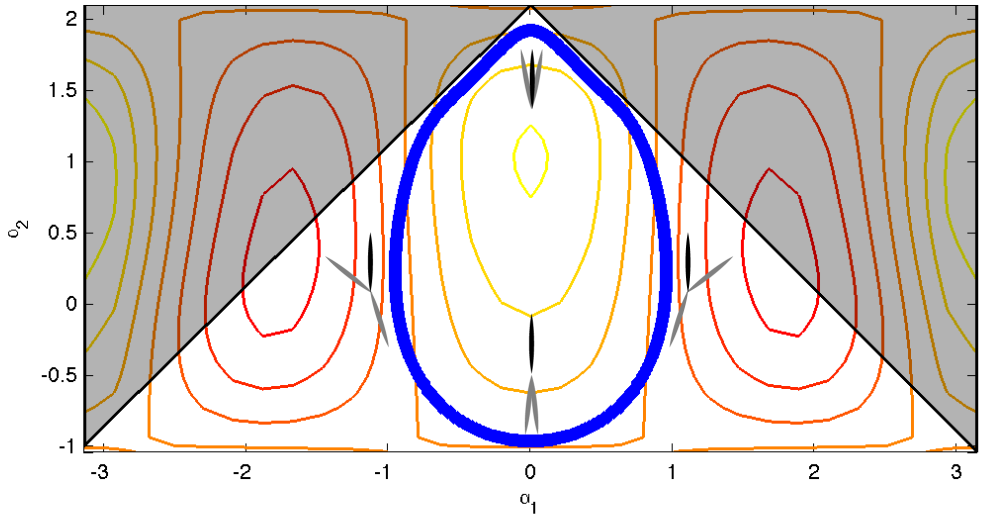

Figure 3-3: Height function for translation is shown by the orange contours. The gait of the rotator is shown with the blue line, moving clockwise in the shape space. The grey area represents impossible configurations.

The optimized translation stroke can be expressed as a Fourier series.

$$\alpha_1(t) = 0.8673\sin(t) + 0.2551\sin(2t) + 0.0680\sin(3t) + 0.0227\sin(4t) \tag{3.4a}$$

$$\alpha_2(t) = 0.7450 - 1.3420\cos(t) - 0.3052\cos(2t) - 0.1017\cos(3t) + 0.0339\cos(4t) \tag{3.4b}$$

This stroke also is non-reciprocal and the swimmer must return to its starting position in a different way than it departed. Again, we can compare this optimized

stroke to the simple stroke proposed above in 3-2. It is found that in this case, the optimized translation stroke produces a translation 1.21 times greater than the simple stroke.

Chapter 4

Conclusion

Defining the geometry and physics of the system using the local connection matrix, and visualizing the system using height functions, the displacement of the swimmer were determined. These height functions were then used to optimize the articulation of Purcell's rotator for two different objective functions - rotation and translation.

The rotation stroke was found to be defined by the zero contour of the height function as well as the physical constraints of the system. The optimized rotation stroke was 1.16 times better at rotating the swimmer than a circular stroke. An optimized translational stroke was also determined. This stroke was less defined by the geometry constraints of the system and was found to be 1.21 times more effective at propelling the swimmer than a simple circular stroke.

Bibliography

[1] Stephen Childress. *Mechanics of swimming and flying*. Cambridge: Cambridge UP, 1981. Print.

[2] R. Dreyfus, J. Baudry, and H.A. Stone. Purcell's "rotator": mechanical rotation at low Reynolds number *The European Physical Journal B* 47: 161-164, 2005.

[3] Jeffery S. Guasto, Roberto Rusconi, and Roman Stocker. Fluid Mechanics of Planktonic Microorganisms. *Annual Review of Fluid Mechanics*. 44: 373-400, 2011.

[4] Ross L. Hatton and Howie Choset. Optimizing Coordinate Choice for Locomoting Systems. *IEEE International Conference on Robotics and Automation*, May 2010.

[5] Ross L. Hatton and Howie Choset. Geometric motion planning: The local connection, stoke's theorem, and the importance of coordinate choice. *International Journal of Robotics Research* 30(8) 988-1014. 2011.

[6] E.M. Purcell. Life at Low Reynolds Numbers. *American Journal of Physics*, 45(1):3-11, 1977.

[7] Daniel Tam and Annete Hosoi. Optimal Stoke Patterns for Purcell's Three-Link Swimmer. *Physical Review Letters*, 2007.